Manufacture Microneedles by 3D Printing

Subjects: Materials Science, Biomaterials

Contributor: Amina Tucak-Smajić

Microneedles (MNs) represent the concept of attractive, minimally invasive puncture devices of micron-sized dimensions that penetrate the skin painlessly and thus facilitate the transdermal administration of a wide range of active substances. MNs have been manufactured by a variety of production technologies, from a range of materials, but most of these manufacturing methods are time-consuming and expensive for screening new designs and making any modifications. Additive manufacturing (AM) has become one of the most revolutionary tools in the pharmaceutical field, with its unique ability to manufacture personalized dosage forms and patient-specific medical devices such as MNs.

Keywords: microneedles ; 3D printing ; transdermal drug delivery ; printing materials ; printing parameters

1. Introduction

Microneedles (MNs) represent skin-friendly puncturing devices of microscale dimensions [1] that are designed to efficiently and painlessly bypass the outermost layer of the skin, the stratum corneum (SC), which acts as a barrier for transdermal penetration of APIs, in particular for those with log p values below 1 and greater than 3 [2], by forming microchannels and thus releasing the drug into the skin's microcirculation [3][4].

Additive manufacturing (AM), commonly known as three-dimensional (3D) printing, rapid prototyping, or solid free form fabrication (SFF), represents a family of techniques launched in the 1980s that revolutionized not only the pharmaceutical industry [5][6] but also the majority of industrial and scientific fields such as automotive [7], aerospace [8], construction [9], and consumer electronics industries [10]. The term "3D printing" was defined by the International Standard Organization (ISO) as "*the fabrication of objects through the deposition of a material using a print head, nozzle, or another printer technology*" [11]. The reason for the great interest in 3D printing was the possibility for fast, cost-effective, and time-saving prototyping of complex structures with high production rates, reduced material waste, and increased productivity [3][12]. More than 10 different AM technologies have been proposed since Chuck Hull's first development and commercialization of stereolithography apparatus (SLA) back in 1986. They include material extrusion, vat photopolymerization, material and binder jetting, powder bed fusion (PBF), directed energy deposition, and sheet lamination [13][14][15], which have been used for the precise manufacture of various drug dosage forms for oral [16][17][18], transdermal [13][14][19][20], vaginal [21], and subcutaneous [22] applications, as well as implants and prosthetics, whose high tunability and complexity are unattainable by conventional techniques [3][6]. More recently, the wide range of 3D printing technologies has opened an interesting new field of research to produce MNs.

2. Microneedles: Characteristics, Classification, and Delivery Strategies

The ultimate success of MN-based drug delivery is founded on the critical parameters, which include their dimensions (shape, size, geometry), manufacturing method, and materials, as well as the type of therapeutics that could be delivered into the skin [23].

According to their structure and design, MN can be "hollow" or "solid", but in the context of their application, MNs can be classified into five categories, hollow, solid, coated, dissolving MNs, and swelling MNs, that can be used for both TDD and extraction of interstitial fluids (**Figure 1**).

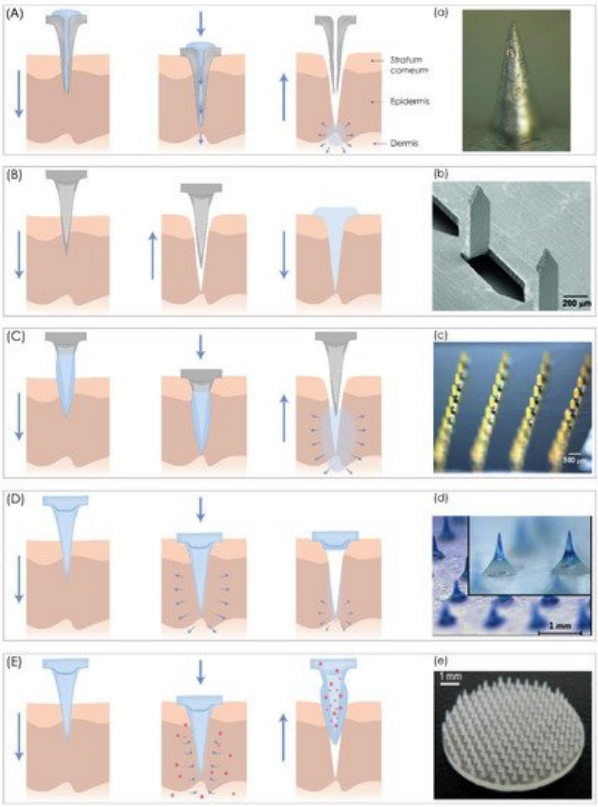

Figure 1. A schematic representation of five different microneedle (MN) types for transdermal drug delivery. (**A**) Hollow MNs puncture the skin and release a liquid drug formulation through the needle lumen. (**B**) Solid MNs create microchannels in the skin and increase drug permeability. (**C**) Coated MNs enable drug dissolution into the skin from the coating film. (**D**) Dissolving MNs release the drug incorporated within the MNs. (**E**) Hydrogel MNs collect interstitial fluids and induce drug release through the swollen microprojections. (**a**) Bright-field microscopy (SZX 16, Olympus, Center Valley, PA, USA) image of hollow MNs. Reproduced with the permission from [24], Springer Nature, 2013. (**b**) SEM microscopy of solid MNs. Reproduced with the permission from [25], Elsevier, Amsterdam, The Netherlands, 2011. (**c**) bright-field microscopy (Olympus SZX12 stereo microscope, Olympus America) image of coated MNs. Reproduced with the permission from [26], Springer Nature, 2007. (**d**) microscope (STC-GE33A, SENTECH, Yokohama, Japan) image of dissolving MNs. Reproduced with the permission from [27], Elsevier, 2013. (**e**) picture of a hydrogel microneedle patch. Reproduced with the permission from [28], John Wiley & Sons—Books, 2015. The image was created with Adobe Illustrator CC (Version 23.0.1.; Adobe Inc., San Jose, CA, USA).

Dissolving MNs are used to slowly release drugs into the skin by the "*poke and release*" approach (**Figure 1**D) [29]. They consist of a soluble matrix containing biodegradable material such as a biodegradable polymer or sugar and encapsulated therapeutic agents in their matrix [2][29][30] and they function according to a one-step application principle [29], as biodegradable MNs dissolve after contact with the interstitial fluid, thus releasing the incorporated drugs [2].

Various materials, including poly(vinyl alcohol) (PVA), poly(vinylpyrrolidone) (PVP), carboxymethyl cellulose (CMC), chondroitin sulfate, and sugars such as dextran, galactose, or maltose have been used to produce this MN type [31][32][33][34][35]. As water-soluble materials are usually used for dissolving MN production, the potential of leaving biohazardous, sharp waste is low, allowing safe disposal of the remaining device [2]. Since the drug release kinetics depend on the degree of dissolution of the incorporated polymers, it is possible to adjust the sustained drug delivery by selecting the proper polymer composition or modifying the manufacturing process [2]. However, the main disadvantage is the deposition of polymers in the skin, which is undesirable for long-term use [2].

Hydrogel MNs are the fifth type of MNs, which consist of a hydrogel-forming matrix [36] and can be used for TDD when a drug is incorporated into cross-linked polymer microprotrusions. They swell after application to the skin, absorb interstitial fluid from the tissue, and subsequently induce drug diffusion through the swollen MNs [2][37]. Usually, they are made from aqueous mixtures of polymeric materials such as polymethylvinylether-co-maleic acid (PMVE/MA) [2]. Besides that, hydrogel MNs are suitable for real-time monitoring of analytes in body fluids as they swell after insertion into the skin and subsequently collect interstitial fluid (**Figure 1**E) [38].

3. Fabrication of Microneedles Using 3D Printing Technologies

The process of 3D printing (3DP) of MNs usually contains three main steps. Firstly, a 3D object is designed with computer-aided design (CAD) software, and the geometry is optimized according to printer specifications. Then, the 3D object is exported to a common and printer-recognizable file format such as standard triangulation language (STL), which includes only 3D geometry in the form of each vertex's position data or an OBJ file in which additional information about polygonal faces or color texture is coded [39]. Finally, the object is printed in a layer-by-layer manner [40].

3.1. Nozzle-Based Deposition Systems

Fused Deposition Modeling (FDM)

One of the most popular AM techniques is extrusion-based fused filament fabrication (FFF), also referred to as fused deposition modeling (FDM). In this process, the suitable thermoplastic material, in the form of a filament, is melted in a liquefier head at a temperature above its melting point and then selectively deposited layer-by-layer through a nozzle on a build plate, where it is cooled and solidified in less than a second, as shown in **Figure 2**. The printer's head moves within the *x*- and *y*-axes, whereas the platform can move within the *z*-axis, thus creating 3D structures [41].

The quality and mechanical properties of the fabricated part can be attributed to the proper selection of process parameters such as nozzle diameter, feed rate, the temperature of both the nozzle and the building plate, printing speed, the height of the layers, and orientation of the built part. All these process parameters need to be studied and optimized in the FDM process to improve surface finish, strength, and other properties of the printed part [42][43].

Initial attempts to use FDM processes in the production of MNs were reported by Luzuriaga et al. (**Figure 2**a). Tang et al. investigated the effects of FDM process parameters, such as printing temperature, layer thickness, extrusion width, infill width, and nozzle orifice diameter on the final print quality of MNs printed with different types of PLA (**Figure 2**c).

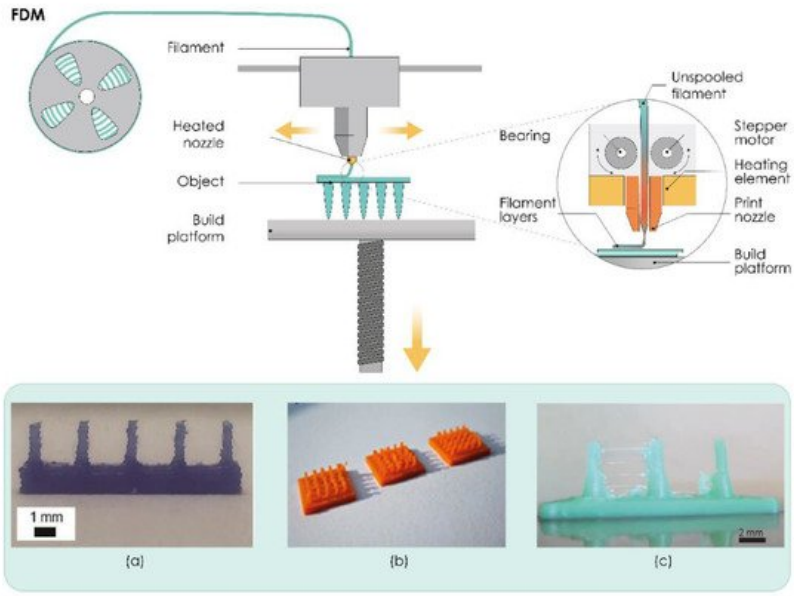

Figure 2. The working principle of fused deposition modeling (FDM). (**a**–**c**) Microneedles produced by FDM technology. Reproduced with permission from [13][19][44], Royal Society of Chemistry, London, UK, 2018 (**a**), Springer Nature, Basingstoke, UK, 2020 (**b**), and John/Wiley & Sons, Inc., Hoboken, NJ, USA, 2020 (**c**). The image was created with Adobe Illustrator CC (Version 23.0.1.; Adobe Inc., San Jose, CA, USA, 2019)

3.2. Laser-Based Writing Systems

3.2.1. Stereolithography (SLA)

Photopolymerization-based or photocuring 3DP technologies, which are based on the ability to selectively polymerize photosensitive polymers through laser emissions or projections of light, are one of the oldest and the most widely used AM technologies in the current manufacturing industry [45]. Vat photopolymerization technologies such as stereolithography (SLA) are liquid-based processes characterized by high precision and accuracy.

SLA printers usually include a printing platform and a resin tank (**Figure 3**). A UV laser draws the cross-section onto a photopolymer resin bath that solidifies the cross-section. Once the first layer is completed, the platform is typically lifted about 0.05–0.15 mm according to the layer thickness [46], the laser then solidifies the next cross-section, and the process

repeats until the entire part is finished. Resin that is not touched by the laser remains in the vat and can be reused. A post-process treatment may be used to achieve the desired mechanical performance [15]. The SLA processes can be divided into two main categories based on different filling mechanisms: free surface and constrained surface. In the free surface approach, structures are built bottom-up from a support platform that rests just below the resin surface while the constrained surface approach, also called the “bat” configuration, has a building platform which can be suspended above the resin bath [47].

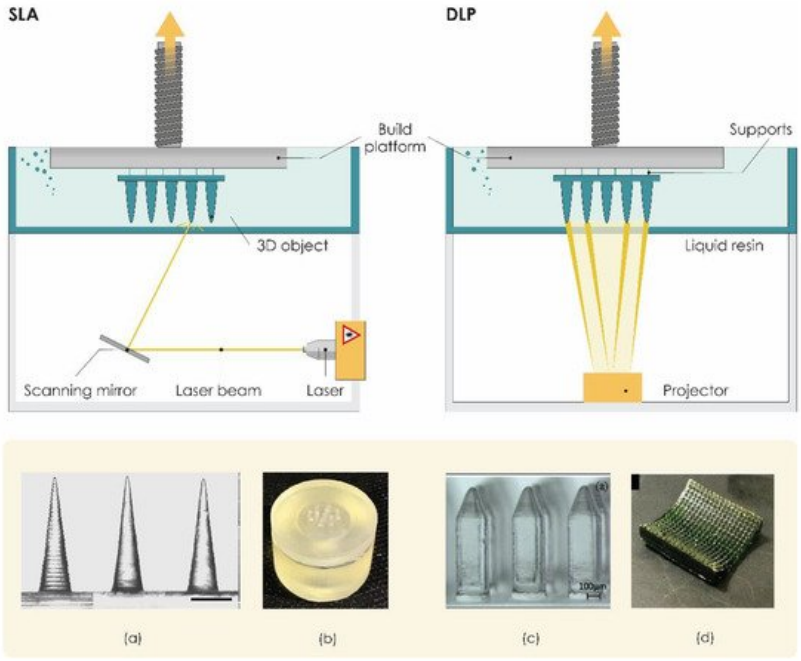

Figure 3. The working principle of stereolithography (SLA) and digital light projection (DLP). (**a**,**b**) Microneedles manufactured by SLA. Reproduced with permission from [48][49], Springer Nature, 2019 and MDPI, 2018. (**c**,**d**) Microneedles manufactured by the DLP technique. Reproduced with permission from [50][51], IOP Publishing, Ltd., Bristol, UK, 2015, 2020 The image was created with Adobe Illustrator CC (Version 23.0.1.; Adobe Inc., San Jose, CA, USA, 2019).

3.2.2. Digital Light Processing (DLP)

Digital light processing (DLP) is photopolymerization-based technology that differs from SLA only in the light source used (**Figure 3**). DLP is usually faster than SLA, as a high-resolution intelligent projector (digital micromirror device, DMD) illuminates the entire cross-section of the object at once in the form of volumetric pixels and the entire layer is produced simultaneously [3]. The technology is characterized by high printing resolution, with a minimum size of 50 µm, and the ability to print objects with a smooth surface. On the other hand, DLP 3D printers are very expensive [40].

3.2.3. Liquid Crystal Display (LCD)

Another vat polymerization technology, namely liquid crystal display (LCD), is based on UV-mediated resin solidification. In LCD 3DP, the liquid crystal display is used as an imaging system. This bottom-up 3D printing method has several advantages over top-down processing, such as the DLP 3DP system includes a smaller volume of resin required during fabrication and has the capability of achieving a high vertical resolution and a shorter curing time (**Figure 4**) [52].

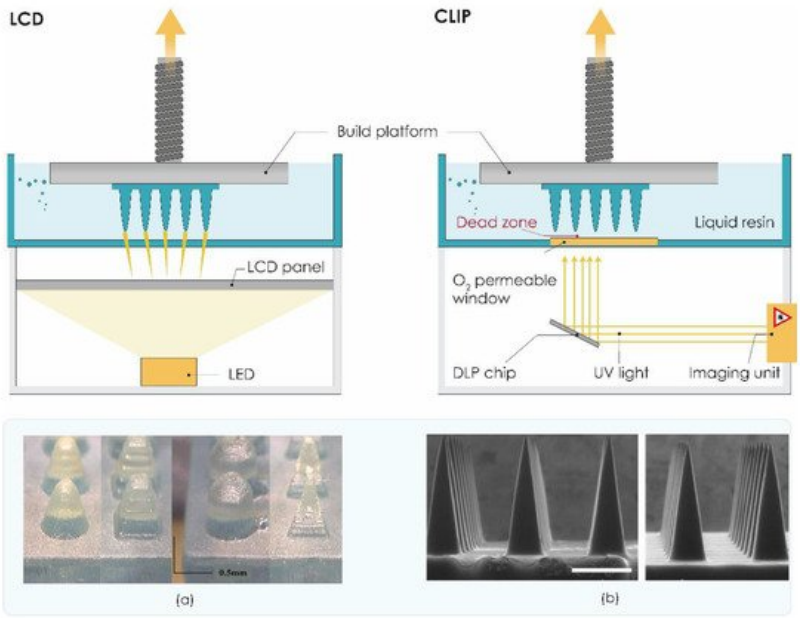

Figure 4. The working principle of liquid crystal display (LCD) and continuous liquid interface production (CLIP). (**a**) Microneedles produced by LCD. Reproduced with permission from [53], Elsevier, 2021 and (**b**) CLIP technology. Reproduced with permission from [54], PLOS, 2016. The image was created with Adobe Illustrator CC (Version 23.0.1.; Adobe Inc., San Jose, CA, USA, 2019).

3.2.4. Continuous Liquid Interface Production (CLIP)

In 2015, Carbon 3D Corp (Redwood, CA, USA) developed new continuous liquid interface production (CLIP) technology as a novel alternative to traditional layer-by-layer SLA [55]. The invention of the oxygen permeation membrane, which helps the consecutive printing for the oxygen permeation to inhibit the radical polymerization, is the key to this technology [40]. The process begins by directing ultraviolet (UV) light through an oxygen-permeable window into a pool of photopolymerizable liquid resin, which is selectively polymerized by UV light. Above the window, a liquid “dead zone” of non-polymerized oxygen-inhibited resin is maintained, enabling continuous rather than layer-by-layer production of the part (**Figure 4**) [56][55]. Although CLIP technology allows fast production of high-resolution structures, the technology is costly and not readily available or convenient for in-house MN manufacture.

Only one year after its introduction, the CLIP technology was successfully used to rapidly prototype MNs for TDD. Johnson et al. utilized the CLIP technique to rapidly manufacture sharp MNs with different geometries in one step (**Figure 4**b). These MN patches have been fabricated from a range of biocompatible materials. Results indicated that CLIP MNs exhibit sufficient strength to pierce murine skin ex vivo and also showed successful delivery of a fluorescent drug surrogate (rhodamine) into the skin [54].

3.2.5. Two-Photon Polymerization (TPP/2PP)

As the most accurate 3DP technology to date, the two-photon polymerization (TPP) or 2PP technique enables layer-by-layer fabrication of 3D structures from solid, liquid, or powder precursors for microscale and nanoscale structures. Induced by a near-infrared femtosecond laser, TPP can fabricate arbitrary and ultraprecise 3D microstructures with high resolution (100 nm lateral resolution and a 300 nm axial resolution) [57]. The technology is based on two-photon absorption. Briefly, a drop of resin is placed on a glass substrate, which is followed by focusing the laser beam of an ultrafast (for example, femtosecond) laser directly on a photosensitive material, so the polymerization process is initiated by two-photon absorption within the focal region (**Figure 5**) [58].

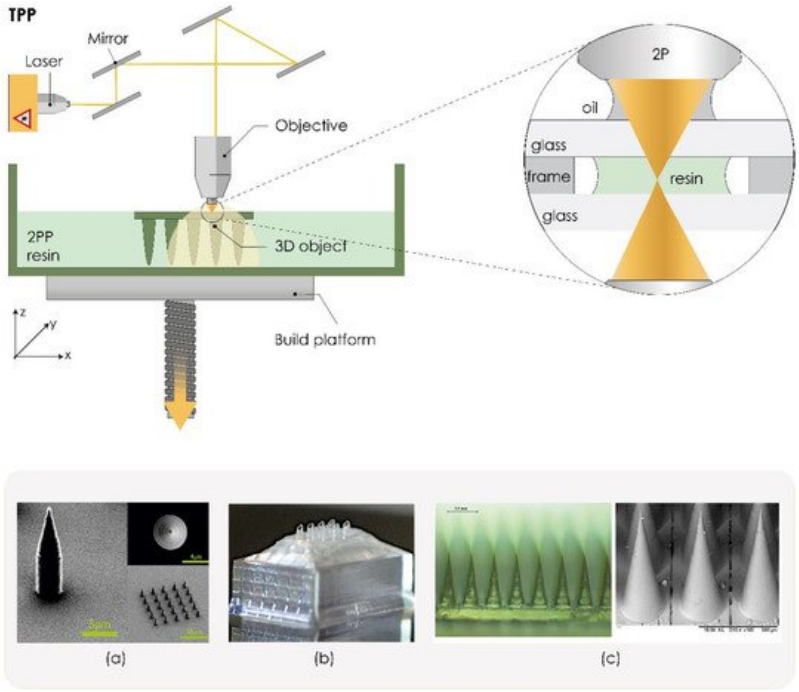

Figure 5. The working principle of two-photon polymerization (TPP) technology. (**a**–**c**) Microneedles produced by TPP. Reproduced with permission from [5][59][60], IOP Publishing, Ltd., 2020, John Wiley & Sons, Inc, 2017, Springer Nature, 2020. The image was created with Adobe Illustrator CC (Version 23.0.1.; Adobe Inc., San Jose, CA, USA, 2019).

3.2.6. Powder Bed Technologies (SLS, DLMS, SLM)

Powders can also be used as materials for 3D printing by applying a high-energy beam in technologies such as selective laser sintering (SLS), selective laser melting (SLM), and direct metal laser sintering (DLMS). These techniques require a high energy flow on the powder bed of building material to produce the desired objects [61], while the solidification process of powders can be achieved by sintering or melting [39].

Selective laser sintering (SLS) is powder bed 3D printing technology invented by Carl R. Deckard for his master's thesis at the University of Texas and was patented in 1989 (US 4863538 patent) [62][63]. This technology produces 3D objects layer-by-layer [64] using a computer-controlled, high-power laser that selectively heats and fuses tightly compact, small powder particles such as metal, plastics, polymers, or ceramics. These particles then solidify and form a 3D structure with the desired shape and properties [39][65][61][66]. Direct metal laser sintering (DMLS) is an extension of the SLS process and produces 3D printed objects by sintering the powdered metals with a precise, high-intensity laser [64]. The SLS and DLMS systems consist of a laser system, powder bed, and spreading platform [66]. In DLMS, the powder bed is filled with metal alloy powders such as bronze, steel, stainless steel 316 L, titanium, or Al-30% Si without a binder or fluxing agent [67]. The 3D process starts with CAD data exported in the industry-standard exchange file format, STL [63]. Subsequently, the powder is distributed uniformly onto the building platform by using a slot feeder and a scraper blade (roller) that even the surface [15][66]. Sintering means that the printing process is maintained at a temperature that does not completely melt the powders, as it is below the melting point of the material, which is sufficient to enable fusion between particles at the molecular level [15][39][63][66]. The powder bed is lowered by the thickness of one layer so that a subsequent layer of powder is loaded into the build tank and fused by the laser. The process is repeated until the final 3D model is created (**Figure 6**) [65][66]. Support during the 3D printing process is provided by unsintered powder particles present on the build platform, which are then removed by hand, a vacuum, or sieving [15][39][66].

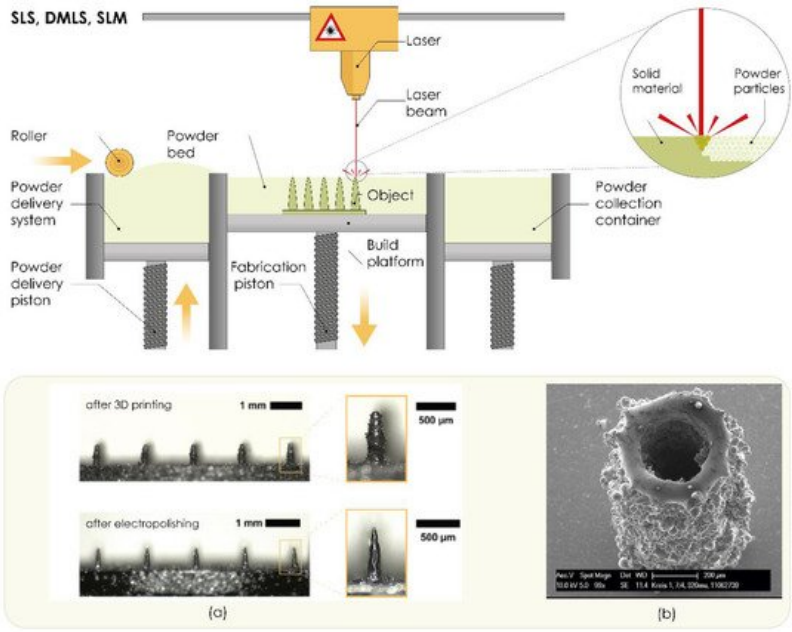

Figure 6. The working principle of powder bed technologies (selective laser sintering, SLS; direct metal laser sintering, DMLS; and selective laser melting, SLM). (**a**) Fabrication of microneedle arrays using DMLS and post-processing by electropolishing. Reproduced with permission from [68], John Wiley & Sons—Books, 2020. (**b**) Fabrication of hollow microneedle using SLM. Reproduced with permission from [69], Walter de Gruyter and Company, Berlin, Germany, 2012. The image was created with Adobe Illustrator CC (Version 23.0.1.; Adobe Inc., San Jose, CA, USA, 2019).

4. Parameters Affecting the Mechanical Properties of 3D Printed Microneedles

4.1. Material Selection

It is well known that materials used for MN manufacturing must have sufficient strength to penetrate biological barriers, must be easily manufactured, and be compatible with drug molecules. Material properties affect critical parameters such as stability, tensile strength, drug loading, and biocompatibility of MNs [70][71]. Biocompatibility and safety are of the utmost importance when it comes to material selection for MN manufacturing. Although the AM technology allows the use of different materials, all materials must fulfill properties such as biocompatibility, biodegradability without toxic products, mechanical strength, and scalability to be used in the development of TDD systems such as MNs [72]. This can seriously limit the expansion of 3D printing in MN manufacturing, as the material selection can be challenging.

4.2. Precision of 3D Printing

In order to achieve the appropriate product quality, a detailed analysis of the impact of all important process parameters is required, regardless of the 3D printing method. Optimization of process parameters is a key criterion for achieving the appropriate product quality in terms of improving dimensional and geometrical accuracy and surface quality [73].

For MN production, printer resolution is one of the most important parameters for achieving the desired MN design and forming sharp MN tips. Print resolution is influenced by the software and hardware components of the device. The mesh density directly affects the print accuracy, so the printing of a model with a fine (denser) mesh is more accurate than the printing of a model with a sparse and uneven mesh. The influence of hardware components is reflected in the quality of manufacturing components of the movement and positioning system (number of increments of stepper motors, quality of production of guides, threaded spindles, belts, etc.), extrusion components, i.e., nozzles, heaters (for extrusion-based techniques), and laser system components (for laser-based techniques).

4.3. Microneedle Design

Regardless of the manufacturing technique, some of the most important characteristics of MNs, such as insertion and penetration behavior, ability to pierce the skin, or the rate of drug delivery, strongly depend on the geometry of MNs, e.g., MN length, base and tip diameter, shape, and interspace (center-to-center spacing) [6][74].

The length of MNs can usually vary between 150 and 2000 µm and guarantees a direct penetration of MNs through the epidermis layer to the capillary system of the skin in dermal tissue [2]. The length of MNs should be carefully optimized

because if the MNs are too long or fragile due to weak materials, the insertion forces can exceed the ultimate tensile forces and cause breaking of the MNs [29][75]. Due to their ability to extract skin interstitial fluid and to monitor numerous biological markers or exogenous molecules, MNs have also been introduced as non-invasive devices for patient monitoring and diagnostics [29][6][37]. For that purpose, the MN length must be at least 900 μm [76].

The 3D printed MNs may also vary depending on their tip or overall shape, as shown in **Figure 7** (e.g., cone, pyramid, cylinder). However, not all 3D printing technologies have the ability to produce all these MN shapes. For example, Luzuriaga et al. and Camović et al. reported that it is quite difficult to obtain a sharp tip of MNs using the FDM method [13][19]. Luzuriaga et al. employed FDM technology to produce MNs with seven different types of shape. Most of them were unable to print because the sharp features exceeded the resolution of the print nozzle, resulting in poor replication of these designs by the 3D printer. Some of the shapes could not be printed due to poor adhesion between extruded layers. As they did not achieve an optimum tip diameter, post-processing in alkaline solution was performed [13]. However, Tang et al. successfully produced a tapered coned MN by the FDM method [44].

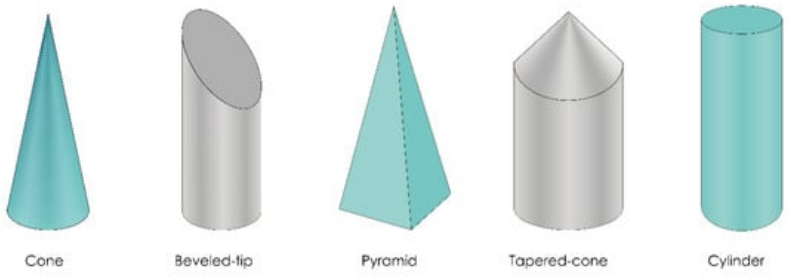

Figure 7. Different shapes of microneedles obtained by 3D printing technologies. The image was created with Adobe Illustrator CC (Version 23.0.1.; Adobe Inc., San Jose, CA, USA, 2019).

5. Evaluation of 3D printed MNs

5.1. Physical Characterization

Geometry, dimensions, surface morphology, and distribution of MNs on the array can be determined and evaluated by visual inspection, stereomicroscopy, and optical or scanning electron microscopy [77]. Properties of the surface of MN patches can be evaluated by drop shape analysis and contact angle determination [53].

Fluorescent labeling or dyeing the molecules incorporated in the MN patch can be used for their identification. Successfully incorporated molecules may be visualized by confocal laser scanning microscopy (CLSM), fluorescent microscopy, or even visual inspection. Visualization is useful for the localization of molecules incorporated within an MN patch whether it is the tip, shaft, or the backing layer [78]. Coated MNs can be evaluated by FTIR spectroscopy [53].

5.2. Mechanical Characterization

Mechanical characterization is necessary to ensure the safe use of MNs. MNs tend to bend, fracture, or buckle due to inelastic or elastic instability during insertion or removal, so it is of great importance to evaluate their mechanical properties. Adequate mechanical strength is required to penetrate the SC and deliver the drug. The term mechanical characterization comprises a range of tests that provide the simulation of MNs' insertion in vivo [2].

5.2.1. Failure Force Tests

Axial Fracture Force Tests

This type of test involves measuring the failure of MNs caused by axial or transverse loading. The test station presses the MN array parallel against a rigid metal surface followed by the measurement of force and displacement while generating the stress against strain curves (**Figure 8**a). If MNs fail, the force drops suddenly and the maximum force applied immediately before the drop is the force of the MNs' failure. Subsequently, MN arrays are visually observed by microscope and compared with scans taken before the failure to determine the failure mode [79]. Axial fracture force tests that use only a single MN should be cautiously interpreted because those results cannot always be correlated with ones taken from an MN array [80].

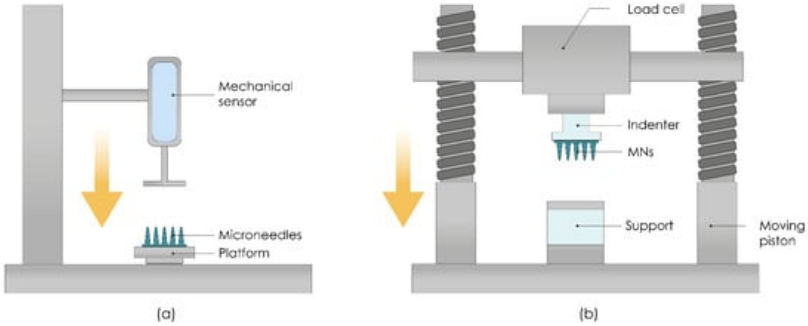

Figure 8. A schematic representation of (**a**) texture analyzer set up for the determination of fracture forces of MN arrays. Reproduced with permission from [81], Elsevier, 2017. (**b**) microneedle penetration testing. Reproduced with permission from [82], Elsevier, 2012. The image was created with Adobe Illustrator CC (Version 23.0.1.; Adobe Inc., San Jose, CA, USA, 2019).

Transverse Fracture Force

Transverse fracture force tests are important for the assessment of the application of MNs, and they can be applied to a single MN, and a row of MNs as well, for which the force should be divided by the number of MNs in a row to calculate the transverse fracture force per individual MN. The main limitation of this test is the required manual alignment of the metal probe with a defined length, which can cause inaccuracies [83].

Baseplate Strength and Flexibility Tests

The degree of flexibility should be sufficient to conform to the irregular topography of the skin without fracturing. To do this, a bending test with three points can be used. Baseplates are placed between two aluminum blocks and the force is applied by a metal probe. The force required to break the baseplate can be measured by observing a maximum peak value on the force–distance curve. The flexibility of the baseplate can be calculated from its bending upon fracture [83].

5.2.2. Insertion Force Tests

Measuring the insertion force required to pierce the skin by MNs is also important to ensure a complete and equivalent assessment of fracture forces. Fracture forces should be significantly higher than the insertion forces required for inserting MNs into the skin. MNs insertion can be done manually or by using different applicators (**Figure 8**b).

5.2.3. Skin Irritation and Recovery Studies

Depending on the size, material, and the type of the delivered drug, mild and transient erythema may occur as a side effect after MN application. The irritation can be observed dermatoscopically or stereomicroscopically. The degree of skin irritation, although subjective and variable, can be determined by the Draize method in which the skin is observed macroscopically before and after the application of MNs and dermatological changes are evaluated according to the degree of erythema and edema [84]. Skin recovery can also be assessed by monitoring changes in the skin over time using digital photographs [6].

5.3. Permeation Studies

5.3.1. In Vitro Permeation Studies

The amount of the drug delivered into the skin can be determined by diffusion cells. Usually, the test is performed on ex vivo human or animal skin or an artificial polymeric membrane placed between receptor and donor compartments. The observed permeant is inserted into the donor compartment, which diffuses into the receptor compartment via the membrane of choice [85]. Transdermal delivery of investigated permeant from MNs can be analyzed from the receptor compartment by high-performance liquid chromatography (HPLC). Intradermal delivery can be examined by extraction and analysis of the compound of interest from the skin sample after permeation [77].

5.3.2. In Vivo Permeation Studies

Neither in vitro nor ex vivo models can fully replicate the in vivo conditions and all skin characteristics. In vivo studies are necessary to investigate the absorption, disposition, and permeation of drugs delivered by MNs. Thickness and elasticity of the skin are crucial parameters that must be considered while selecting the appropriate in vivo model.

Another important factor to consider when developing in vivo models for MN performance assessments is the application site. Different anatomical sites offer a varying extent of permeability and barrier function of the skin. In addition, the thickness and rigidness of the injection site, which can be affected by lymphatic uptake, play an important role in achieving reproducible results. Measuring plasma levels of tested drugs provides information about their transdermal delivery from MNs, while skin extraction provides information about intradermal delivery. In vivo permeation studies can also provide information about the metabolism of delivered drugs [77].

6. Conclusions

The unprecedented ease with which complex objects are produced and the relatively low price of commercially available 3D printers have given 3D printing significant popularity and has been spoken of as a third industrial revolution. It has the inherent ability to revolutionize conventional pharmaceutical manufacturing by adjusting the size, shape, and release profile of different drug delivery systems, allowing the precise preparation of personalized dosage forms to address individual patient needs. This technology can play a very important role in the manufacture of personalized TDD systems, as evidenced by the growing interest in the 3D printing of MNs. MNs represent next-generation therapeutic systems that may have a notable impact on clinical medicine in the future, but further multidisciplinary research is needed to obtain ideal MN-based point-of-care systems. Having in mind that AM can be used to rapidly prototype different MN designs as well as MN-based TDD, this approach will undoubtedly optimize the effectiveness of these delivery systems and open new horizons for researchers in the field. Even though photopolymerization-based technologies have been the most widely used 3DP technology in the production of MNs, there is also great potential in all other technologies. However, clinical translation and commercial development of 3DP MNs are still a challenge, and a lot of future work is needed, especially in material selection, optimization of printing and post-printing parameters, and drug loading approaches.

Further investigations are needed to find relationships between MN design and printing parameters and their quality and performance. In addition, future studies need to focus on improving printer properties, such as the laser beam in laser-based methods or nozzle features in extrusion-based methods, to develop faster methods with the highest resolution. Standardized evaluation methods and testing protocols for 3DP MNs also need to be further developed as the variety of mechanical equipment used gives divergent results that are sometimes very difficult to compare. Advances in 3D printing techniques for MN production, as well as recent breakthroughs in electronic mechanicals and artificial intelligence, offer enormous potential for the development of TDD systems that would allow patients to self-administer drugs such as vaccines.

References

1. Hong, X.; Wu, Z.; Chen, L.; Wu, F.; Wei, L.; Yuan, W. Hydrogel Microneedle Arrays for Transdermal Drug Delivery. Nano-Micro Lett. 2014, 6, 191–199.
2. Larrañeta, E.; Lutton, R.E.M.; Woolfson, A.D.; Donnelly, R.F. Microneedle arrays as transdermal and intradermal drug delivery systems: Materials science, manufacture and commercial development. Mater. Sci. Eng. R Rep. 2016, 104, 1–32.
3. Economidou, S.N.; Lamprou, D.A.; Douroumis, D. 3D printing applications for transdermal drug delivery. Int. J. Pharm. 2018, 544, 415–424.
4. Tucak, A.; Sirbubalo, M.; Hindija, L.; Rahić, O.; Hadžiabdić, J.; Muhamedagić, K.; Čekić, A.; Vranić, E. Microneedles: Characteristics, Materials, Production Methods and Commercial Development. Micromachines 2020, 11, 961.
5. Cordeiro, A.S.; Tekko, I.A.; Jomaa, M.H.; Vora, L.; McAlister, E.; Volpe-zanutto, F.; Nethery, M.; Baine, P.T.; Mitchell, N.; Mcneill, D.W.; et al. Two-Photon Polymerisation 3D Printing of Microneedle Array Templates with Versatile Designs: Application in the Development of Polymeric Drug Delivery Systems. Pharm. Res. 2020, 37, 1–15.
6. Wu, M.; Zhang, Y.; Huang, H.; Li, J.; Liu, H.; Guo, Z.; Xue, L.; Liu, S.; Lei, Y. Assisted 3D printing of microneedle patches for minimally invasive glucose control in diabetes. Mater. Sci. Eng. C 2020, 117, 111299.
7. Richardson, M. Designer/Maker: The Rise of Additive Manufacturing, Domestic-Scale Production and the Possible Implications for the Automotive Industry. Comput. Aided. Des. Appl. 2012, PACE, 33–48.
8. Ahmed, N.A.; Page, J.R. Manufacture of an unmanned aerial vehicle (UAV) for advanced project design using 3D printing technology. In Proceedings of the Applied Mechanics and Materials; Trans Tech Publications Ltd.: Bäch SZ, Switzerland, 2013; Volume 397–400, pp. 970–980.

9. Henke, K.; Treml, S. Wood based bulk material in 3D printing processes for applications in construction. Eur. J. Wood P rod. 2013, 71, 139–141.
10. MacDonald, E.; Salas, R.; Espalin, D.; Perez, M.; Aguilera, E.; Muse, D.; Wicker, R.B. 3D printing for the rapid prototypi ng of structural electronics. IEEE Access 2014, 2, 234–242.
11. International Organization for Standardization. ISO/ASTM 52900: Additive Manufacturing-General Principles-Terminolo gy; ISO/ASME International: Geneva, Switzerland, 2015; Volume 5, pp. 1–26.
12. Goole, J.; Amighi, K. 3D printing in pharmaceutics: A new tool for designing customized drug delivery systems. Int. J. P harm. 2016, 499, 376–394.
13. Luzuriaga, M.A.; Berry, D.R.; Reagan, J.C.; Smaldone, R.A.; Gassensmitha, J.J. Biodegradable 3D printed polymer mic roneedles for transdermal drug delivery. Lab Chip 2018, 18, 1223–1230.
14. Lim, S.H.; Kathuria, H.; Tan, J.J.Y.; Kang, L. 3D printed drug delivery and testing systems—a passing fad or the future? Adv. Drug Deliv. Rev. 2018, 132, 139–168.
15. Ngo, T.D.; Kashani, A.; Imbalzano, G.; Nguyen, K.T.Q.; Hui, D. Additive manufacturing (3D printing): A review of materia ls, methods, applications and challenges. Compos. Part B 2018, 143, 172–196.
16. Maroni, A.; Melocchi, A.; Parietti, F.; Foppoli, A.; Zema, L.; Gazzaniga, A. 3D printed multi-compartment capsular device s for two-pulse oral drug delivery. J. Control. Release 2017, 268, 10–18.
17. Melocchi, A.; Parietti, F.; Loreti, G.; Maroni, A.; Gazzaniga, A.; Zema, L. 3D printing by fused deposition modeling (FD M) of a swellable/erodible capsular device for oral pulsatile release of drugs. J. Drug Deliv. Sci. Technol. 2015, 30, 360–367.
18. Goyanes, A.; Wang, J.; Buanz, A.; Martínez-Pacheco, R.; Telford, R.; Gaisford, S.; Basit, A.W. 3D Printing of Medicines: Engineering Novel Oral Devices with Unique Design and Drug Release Characteristics. Mol. Pharm. 2015, 12, 4077–4 084.
19. Camović, M.; Biščević, A.; Brčić, I.; Borčak, K.; Bušatlić, S.; Ćenanović, N.; Dedović, A.; Mulalić, A.; Osmanlić, M.; Sirbu balo, M.; et al. Coated 3D Printed PLA Microneedles as Transdermal Drug Delivery Systems. In Proceedings of the CM BEBIH 2019. IFMBE Proceedings; Badnjević, A., Škrbić, R., Gurbeta Pokvić, L., Eds.; Springer Nature: Cham, Switzerl and, 2020; Volume 73, pp. 735–742.
20. Pere, C.P.P.; Economidou, S.N.; Lall, G.; Ziraud, C.; Boateng, J.S.; Alexander, B.D.; Lamprou, D.A.; Douroumis, D. 3D printed microneedles for insulin skin delivery. Int. J. Pharm. 2018, 544, 425–432.
21. Fu, J.; Yu, X.; Jin, Y. 3D printing of vaginal rings with personalized shapes for controlled release of progesterone. Int. J. Pharm. 2018, 539, 75–82.
22. Gowers, S.A.N.; Curto, V.F.; Seneci, C.A.; Wang, C.; Anastasova, S.; Vadgama, P.; Yang, G.Z.; Boutelle, M.G. 3D Print ed Microfluidic Device with Integrated Biosensors for Online Analysis of Subcutaneous Human Microdialysate. Anal. Ch em. 2015, 87, 7763–7770.
23. Guillot, A.J.; Cordeiro, A.S.; Donnelly, R.F.; Montesinos, M.C.; Garrigues, T.M.; Melero, A. Microneedle-based delivery: An overview of current applications and trends. Pharmaceutics 2020, 12, 569.
24. Norman, J.J.; Choi, S.O.; Tong, N.T.; Aiyar, A.R.; Patel, S.R.; Prausnitz, M.R.; Allen, M.G. Hollow microneedles for intra dermal injection fabricated by sacrificial micromolding and selective electrodeposition. Biomed. Microdevices 2013, 15, 203–210.
25. Gupta, J.; Gill, H.S.; Andrews, S.N.; Prausnitz, M.R. Kinetics of skin resealing after insertion of microneedles in human subjects. J. Control. Release 2011, 154, 148–155.
26. Gill, H.S.; Prausnitz, M.R. Coating formulations for microneedles. Pharm. Res. 2007, 24, 1369–1380.
27. Kim, J.D.; Kim, M.; Yang, H.; Lee, K.; Jung, H. Droplet-born air blowing: Novel dissolving microneedle fabrication. J. Co ntrol. Release 2013, 170, 430–436.
28. Yang, S.; Wu, F.; Liu, J.; Fan, G.; Welsh, W.; Zhu, H.; Jin, T. Phase-Transition Microneedle Patches for Efficient and Ac curate Transdermal Delivery of Insulin. Adv. Funct. Mater. 2015, 25, 4633–4641.
29. Nagarkar, R.; Singh, M.; Nguyen, H.X.; Jonnalagadda, S. A review of recent advances in microneedle technology for tra nsdermal drug delivery. J. Drug Deliv. Sci. Technol. 2020, 59, 101923.
30. Van Der Maaden, K.; Jiskoot, W.; Bouwstra, J. Microneedle technologies for (trans)dermal drug and vaccine delivery. J. Control. Release 2012, 161, 645–655.
31. Ito, Y.; Hagiwara, E.; Saeki, A.; Sugioka, N.; Takada, K. Feasibility of microneedles for percutaneous absorption of insuli n. Eur. J. Pharm. Sci. 2006, 29, 82–88.

32. Kathuria, H.; Kang, K.; Cai, J.; Kang, L. Rapid microneedle fabrication by heating and photolithography. Int. J. Pharm. 2020, 575, 118992.

33. Wilke, N.; Mulcahy, A.; Ye, S.R.; Morrissey, A. Process optimization and characterization of silicon microneedles fabricated by wet etch technology. Microelectron. J. 2005, 36, 650–656.

34. Liu, Y.; Eng, P.F.; Guy, O.J.; Roberts, K.; Ashraf, H.; Knight, N. Advanced deep reactive-ion etching technology for hollow microneedles for transdermal blood sampling and drug delivery. IET Nanobiotechnology 2013, 7, 59–62.

35. Camović, M.; Biščević, A.; Brčić, I.; Borčak, K.; Bušatlić, S.; Ćenanović, N.; Dedović, A.; Mulalić, A.; Sirbubalo, M.; Tucak, A.; et al. Acid-resistant capsules with sugar microneedles for oral delivery of ascorbic acid. In Proceedings of the CMBEBIH 2019. IFMBE Proceedings; Badnjević, A., Škrbić, R., Gurbeta Pković, L., Eds.; Springer: Cham, Switzerland, 2019; pp. 749–753.

36. Donnelly, R.F.; Raj Singh, T.R.; Woolfson, A.D. Microneedle-based drug delivery systems: Microfabrication, drug delivery, and safety. Drug Deliv. 2010, 17, 187–207.

37. Vranić, E.; Tucak, A.; Sirbubalo, M.; Rahić, O.; Elezović, A.; Hadžiabdić, J. Microneedle-based sensor systems for real-time continuous transdermal monitoring of analytes in body fluids. In Proceedings of the CMBEBIH 2019, IFMBE Proceedings; Badnjević, A., Škrbić, R., Gurbeta Pković, L., Eds.; Springer: Cham, Switzerland, 2019; pp. 167–172.

38. Donnelly, R.F.; McCrudden, M.T.C.; Alkilani, A.Z.; Larrañeta, E.; McAlister, E.; Courtenay, A.J.; Kearney, M.C.; Raj Singh, T.R.; McCarthy, H.O.; Kett, V.L.; et al. Hydrogel-forming microneedles prepared from “super swelling” polymers combined with lyophilised wafers for transdermal drug delivery. PLoS ONE 2014, 9.

39. Jamróz, W.; Szafraniec, J.; Kurek, M.; Jachowicz, R. 3D Printing in Pharmaceutical and Medical Applications–Recent Achievements and Challenges. Pharm. Res. 2018, 35, 176.

40. Quan, H.; Zhang, T.; Xu, H.; Luo, S.; Nie, J.; Zhu, X. Photo-curing 3D printing technique and its challenges. Bioact. Mater. 2020, 5, 110–115.

41. Carneiro, O.S.; Silva, A.F.; Gomes, R. Fused deposition modeling with polypropylene. Mater. Des. 2015, 83, 768–776.

42. Mohamed, O.A.; Masood, S.H.; Bhowmik, J.L. Optimization of fused deposition modeling process parameters: A review of current research and future prospects. Adv. Manuf. 2015, 3, 42–53.

43. Camposeco-Negrete, C. Optimization of printing parameters in fused deposition modeling for improving part quality and process sustainability. Int. J. Adv. Manuf. Technol. 2020, 108, 2131–2147.

44. Tang, T.O.; Holmes, S.; Dean, K.; Simon, G.P. Design and fabrication of transdermal drug delivery patch with milliprojections using material extrusion 3D printing. J. Appl. Polym. Sci. 2020, 137, 1–17.

45. ASTM Committee. F42 ISO/ASTM 52921-2013: Standard Terminology for Additive Manufacturing-Coordinate Systems and Test Methodologies. ASTM Int. 2013, 1, 1–13.

46. Rahmati, S.; Ghadami, F. Process Parameters Optimization to Improve Dimensional Accuracy of Stereolithography Parts. Int. J. Adv. Des. Manuf. Technol. 2014, 7, 59–65.

47. Schmidleithner, C.; Kalaskar, D.M. Stereolithography. In 3D Printing; Cvetković, D., Ed.; InTech: London, UK, 2018; pp. 3–22.

48. Krieger, K.J.; Bertollo, N.; Dangol, M.; Sheridan, J.T.; Lowery, M.M.; O’Cearbhaill, E.D. Simple and customizable method for fabrication of high-aspect ratio microneedle molds using low-cost 3D printing. Microsyst. Nanoeng. 2019, 5, 42.

49. Farias, C.; Lyman, R.; Hemingway, C.; Chau, H.; Mahacek, A.; Bouzos, E.; Mobed-Miremadi, M. Three-dimensional (3D) printed microneedles for microencapsulated cell extrusion. Bioengineering 2018, 5, 59.

50. Lu, Y.; Mantha, S.N.; Crowder, D.C.; Chinchilla, S.; Shah, K.N.; Yun, Y.H.; Wicker, R.B.; Choi, J.W. Microstereolithography and characterization of poly(propylene fumarate)-based drug-loaded microneedle arrays. Biofabrication 2015, 7, 045001.

51. Lim, S.H.; Tiew, W.J.; Zhang, J.; Ho, P.C.L.; Kachouie, N.N.; Kang, L. Geometrical optimisation of a personalised microneedle eye patch for transdermal delivery of anti-wrinkle small peptide. Biofabrication 2020, 12.

52. Mohamed, M.; Kumar, H.; Wang, Z.; Martin, N.; Mills, B.; Kim, K. Rapid and Inexpensive Fabrication of Multi-Depth Microfluidic Device using High-Resolution LCD Stereolithographic 3D Printing. J. Manuf. Mater. Process. 2019, 3, 26.

53. Xenikakis, I.; Tsongas, K.; Tzimtzimis, E.K.; Zacharis, C.K.; Theodoroula, N.; Kalogianni, E.P.; Demiri, E.; Vizirianakis, I.S.; Tzetzis, D.; Fatouros, D.G. Fabrication of hollow microneedles using liquid crystal display (LCD) vat polymerization 3D printing technology for transdermal macromolecular delivery. Int. J. Pharm. 2021, 597, 120303.

54. Johnson, A.R.; Caudill, C.L.; Tumbleston, J.R.; Bloomquist, C.J.; Moga, K.A.; Ermoshkin, A.; Shirvanyants, D.; Mecham, S.J.; Luft, J.C.; De Simone, J.M. Single-step fabrication of computationally designed microneedles by continuous liquid interface production. PLoS ONE 2016, 11, 1–17.

55. Tumbleston, J.R.; Shirvanyants, D.; Ermoshkin, N.; Janusziewicz, R.; Johnson, A.R.; Kelly, D.; Chen, K.; Pinschmidt, R.; Rolland, J.P.; Ermoshkin, A.; et al. Continuous liquid interface production of 3D objects. Science 2015, 347, 1349–1352.

56. Balli, J.; Kumpaty, S.; Anewenter, V. Continuous liquid interface production of 3D objects: An unconventional technology and its challenges and opportunities. In Proceedings of the ASME International Mechanical Engineering Congress and Exposition, Proceedings (IMECE); American Society of Mechanical Engineers (ASME): New York, NY, USA, 2017; Volume 5.

57. Xing, J.F.; Zheng, M.L.; Duan, X.M. Two-photon polymerization microfabrication of hydrogels: An advanced 3D printing technology for tissue engineering and drug delivery. Chem. Soc. Rev. 2015, 44, 5031–5039.

58. Farsari, M.; Chichkov, B.N. Materials processing: Two-photon fabrication. Nat. Photonics 2009, 3, 450–452.

59. Kavaldzhiev, M.; Perez, J.E.; Ivanov, Y.; Bertoncini, A.; Liberale, C.; Kosel, J. Biocompatible 3D printed magnetic micro needles. Biomed. Phys. Eng. Express 2017, 3, 025005.

60. Moussi, K.; Bukhamsin, A.; Hidalgo, T.; Kosel, J. Biocompatible 3D Printed Microneedles for Transdermal, Intradermal, and Percutaneous Applications. Adv. Eng. Mater. 2020, 22, 1901358.

61. Beg, S.; Almalki, W.H.; Malik, A.; Farhan, M.; Aatif, M.; Rahman, Z.; Alruwaili, N.K.; Alrobaian, M.; Tarique, M.; Rahman, M. 3D printing for drug delivery and biomedical applications. Drug Discov. Today 2020, 25, 1668–1681.

62. Deckard, C.R..; Beaman, J.J..; Darrah, J.F. Method and Apparatus for Producing Parts by Selective Sintering. U.S. Patent 4,863,538, 5 September 1989.

63. Mazzoli, A. Selective laser sintering in biomedical engineering. Med. Biol. Eng. Comput. 2013, 51, 245–256.

64. Singh, R.; Singh, S.; Hashmi, M.S.J. Implant Materials and Their Processing Technologies; Elsevier Ltd.: Amsterdam, The Netherlands, 2016; ISBN 9780128035818.

65. Gardan, J. Additive manufacturing technologies: State of the art and trends. Int. J. Prod. Res. 2016, 54, 3118–3132.

66. Charoo, N.A.; Barakh Ali, S.F.; Mohamed, E.M.; Kuttolamadom, M.A.; Ozkan, T.; Khan, M.A.; Rahman, Z. Selective laser sintering 3D printing–an overview of the technology and pharmaceutical applications. Drug Dev. Ind. Pharm. 2020, 46, 869–877.

67. Rahmati, S. 10.12. Direct Rapid Tooling. In Comprehensive Materials Processing; Hashmi, S., Batalha, G., Van Tyne, C., Yilbas, B., Eds.; Elsevier: Amsterdam, The Netherlands, 2014; Volume 10, pp. 303–344. ISBN 9780080965338.

68. Krieger, K.J.; Liegey, J.; Cahill, E.M.; Bertollo, N.; Lowery, M.M.; O'Cearbhaill, E.D. Development and Evaluation of 3D-Printed Dry Microneedle Electrodes for Surface Electromyography. Adv. Mater. Technol. 2020, 5, 1–13.

69. Gieseke, M.; Senz, V.; Vehse, M.; Fiedler, S.; Irsig, R.; Hustedt, M.; Sternberg, K.; Nölke, C.; Kaierle, S.; Wesling, V.; et al. Additive manufacturing of drug delivery systems. Biomed. Tech. 2012, 57, 398–401.

70. Bhatnagar, S.; Gadeela, P.R.; Thathireddy, P.; Venuganti, V.V.K. Microneedle-based drug delivery: Materials of construction. J. Chem. Sci. 2019, 131.

71. Ali, R.; Mehta, P.; Arshad, M.; Kucuk, I.; Chang, M.W.; Ahmad, Z. Transdermal Microneedles—A Materials Perspective. AAPS PharmSciTech 2020, 21.

72. Lee, K.J.; Jeong, S.S.; Roh, D.H.; Kim, D.Y.; Choi, H.K.; Lee, E.H. A practical guide to the development of microneedle systems–In clinical trials or on the market. Int. J. Pharm. 2020, 573, 118778.

73. Lee, P.; Chung, H.; Won Lee, S.; Yoo, J.; Ko, J. Review: Dimensional accuracy in additive manufacturing processes. In Proceedings of the ASME 2014 International Manufacturing Science and Engineering Conference, Detroit, MI, USA, 9–13 June 2014; pp. 1–8.

74. Kjar, A.; Huang, Y. Application of micro-scale 3D printing in pharmaceutics. Pharmaceutics 2019, 11, 390.

75. Economidou, S.N.; Pissinato Pere, C.P.; Okereke, M.; Douroumis, D. Optimisation of Design and Manufacturing Parameters of 3D Printed Solid Microneedles for Improved Strength, Sharpness, and Drug Delivery. Micromachines 2021, 12, 117.

76. Ovsianikov, A.; Chichkov, B.; Mente, P.; Monteiro-Riviere, N.A.; Doraiswamy, A.; Narayan, R.J. Two photon polymerization of polymer-ceramic hybrid materials for transdermal drug delivery. Int. J. Appl. Ceram. Technol. 2007, 4, 22–29.

77. Sabri, A.H.; Kim, Y.; Marlow, M.; Scurr, D.J.; Segal, J.; Banga, A.K.; Kagan, L.; Lee, J.B. Intradermal and transdermal drug delivery using microneedles–Fabrication, performance evaluation and application to lymphatic delivery. Adv. Drug Deliv. Rev. 2020, 153, 195–215.

78. Van Der Maaden, K.; Sekerdag, E.; Schipper, P.; Kersten, G.; Jiskoot, W.; Bouwstra, J. Layer-by-Layer Assembly of Inactivated Poliovirus and N-Trimethyl Chitosan on pH-Sensitive Microneedles for Dermal Vaccination. Langmuir 2015, 31,

8654–8660.

79. Park, J.-H.; Allen, M.G.; Prausnitz, M.R. Biodegradable polymer microneedles: Fabrication, mechanics and transdermal drug delivery. J. Control. Release 2005, 104, 51–66.
80. Davis, S.P.; Landis, B.J.; Adams, Z.H.; Allen, M.G.; Prausnitz, M.R. Insertion of microneedles into skin: Measurement a nd prediction of insertion force and needle fracture force. J. Biomech. 2004, 37, 1155–1163.
81. Machekposhti, S.; Soltani, M.; Najafizadeh, P.; Ebrahimi, S.A.; Chen, P. Biocompatible polymer microneedle for topical/ dermal delivery of tranexamic acid. J. Control. Release 2017, 261, 87–92.
82. Ryan, E.; Garland, M.J.; Singh, T.R.R.; Bambury, E.; O'Dea, J.; Migalska, K.; Gorman, S.P.; McCarthy, H.O.; Gilmore, B.F.; Donnelly, R.F. Microneedle-mediated transdermal bacteriophage delivery. Eur. J. Pharm. Sci. 2012, 47, 297–304.
83. Donnelly, R.F.; Majithiya, R.; Singh, T.R.R.; Morrow, D.I.J.; Garland, M.J.; Demir, Y.K.; Migalska, K.; Ryan, E.; Gillen, D.; Scott, C.J.; et al. Design, optimization and characterisation of polymeric microneedle arrays prepared by a novel laser-based micromoulding technique. Pharm. Res. 2011, 28, 41–57.
84. Kusamori, K.; Katsumi, H.; Sakai, R.; Hayashi, R.; Hirai, Y.; Tanaka, Y.; Hitomi, K.; Quan, Y.-S.; Kamiyama, F.; Yamada, K.; et al. Development of a drug-coated microneedle array and its application for transdermal delivery of interferon alph a. Biofabrication 2016, 8, 15006.
85. Gupta, J.; Gupta, R. Vanshita Microneedle Technology: An Insight into Recent Advancements and Future Trends in Dru g and Vaccine Delivery. Assay Drug Dev. Technol. 2021, 19, 97–114.
